

Non-Contact Boundary Layer Profiler using Low-Coherence Self-Referencing Velocimetry

Andreas Kempe¹, Stefan Schlamp², Thomas Rösgen³

1: Institute of Fluid Dynamics, ETH Zurich, Switzerland, kempe@ifd.mavt.ethz.ch

2: Institute of Fluid Dynamics, ETH Zurich, Switzerland, schlamp@ifd.mavt.ethz.ch

3: Institute of Fluid Dynamics, ETH Zurich, Switzerland, roesgen@ifd.mavt.ethz.ch

Abstract: A spatially self-referencing velocimetry system based on low-coherence interferometry has been developed. The measurement technique is contactless, it relies on the interference between back-reflected light from an arbitrary reference surface and from particles in the flow. Due to the measurement principle, the absolute spatial accuracy and the spatial resolution only depend on the coherence length of the light source. Normally this is a superluminescent diode with a coherence length of tens of microns. Thus the system's primary use might be seen in boundary layer measurements, i.e., taking an object surface as reference.

Two approaches with very similar experimental setups are demonstrated – one based on the Doppler effect, the other on time-of-flight measurements. The measurement location is always given relative to an arbitrary reference surface (e.g. a moving body). Scanning of the measurement location along the beam direction does not require mechanical movement of the sensor head. The first approach measures velocities relative to the reference surface, the second relative to the sensor head.

The presented prototype is an all-fiber assembly. Optical fibers of arbitrary lengths connect the self-contained optical and electronics setup to the sensor head. Proof-of-principle measurements for two generic flows (Poiseuille and Taylor-Couette flow) are reported in this paper.

1. Introduction

Velocimetry techniques for boundary layer measurements face two challenges: spatial resolution and non-intrusiveness. In most technical applications, the thickness of the boundary layers is on the order of 1 mm such that sub-millimeter resolution is required for meaningful measurements. The requirements are even higher when the viscous sub-layer and the log-layer have to be resolved (Schlichting and Gersten 2000).

Traditionally, hot-wire anemometry (or constant temperature anemometry, CTA) has been the method of choice for such measurements (e.g., Häggmark et al. 2000, Wolff et al. 2000, Ligrani and Bradshaw 1987). The typical diameter of the wire is on the order of micrometers. They are typically 1-2 mm long, but the spatial resolution in the wall-parallel direction is not critical. Because the measurement location is identical to the probe location, the probe has to be moved to obtain the velocity profile across the boundary layer. This also makes this technique problematic for measurements over moving objects. Recently, micro-PIV has been applied to high-resolution boundary layer measurements. PIV either requires optical access from at least two directions (one for the illuminating laser sheet, the second for the camera) or a depth resolving focusing optic as in microscopy (Lin and Perlin 1998, Meinhart et al. 2000). Depending on the geometry and the object's movement, this might not be feasible. Laser-Doppler velocimetry (LDV), to which the proposed technique is most similar, lacks the required spatial resolution, which is determined by the diameter of the intersecting laser beams and the crossing angle. LDV measures the velocity component perpendicular to the long axis of the intersection ellipsoid. This means that the spatial resolution is poorest in the direction where it is most critical. With a tilted fringe system or the use of low-coherent light this intersection volume can also be resolved in the order of microns (Büttner and Czarske 2003, Büttner and Czarske 2001).

In a PIV image, the flow is visible together with the object such that it can be possible to deduce the measurement location (relative to the surface) from the data without independent knowledge of the object's trajectory. CTA and LDV, on the other hand, are not self-referencing. At any instance, the relative location of the object to the measurement volume has to be known. If the motion is irregular or if the shape of the object changes over time, this might pose a problem in itself.

The new technique is self-referencing with respect to its vertical measurement location and has a spatial resolution of typically 30 micrometer. It measures in-plane components and the out-of-plane component of the velocity vector. The sensitivity to out-of plane velocities (which are typically much lower) is tenfold (typical value, which can be adjusted) higher than for in-plane velocities. As for LDV and PIV, particle seeding is required. Conceptually, planar measurements (cf. Particle Imaging Velocimetry PIV) are also possible with self-referencing capabilities.

The working principle of this new technique is explained using the example of a three-component boundary layer profiler. It relies on the Doppler effect, but a very similar experimental setup allows velocimetry based on the laser-two-focus principle. The latter approach is described only briefly and data is just presented for comparison with the former method. Both systems are spatially self-referenced relative to a surface, but applications where the sensor head is the reference follow the same principle. We want to introduce a notation for the new approach with "SR" standing for self-referencing, i.e., SR-LDV, SR-L2F, etc.

2. Measurement principle SR-LDV

Fig.1 shows the schematic setup of the optical components in the interferometer unit of the system. A superluminescent diode (SLD, Superlum Diodes Model SLD56-HP2, 10 mW) emits low-coherence light into a single-mode fiber. A fiber-optical isolator protects the sensitive light source from back-reflections and guides the light to a polarization insensitive optical circulator. The circulator is used to transfer the light through a single-mode optical fiber to the sensor front end (SFE), where a lens couples the light out of the fiber and into the measurement volume.

A fraction of the incident light is reflected back from the surface of the test object onto the lens and back into the fiber towards the circulator, where it is deflected into the interferometer. A small fraction of the light is also reflected off the particles passing the laser beam. Following the nomenclature of Fig. 2, light reflected off the test object surface is denoted as rays 1a and 1b and the light scattered off the particles in the flow is denoted as rays 2a and 2b (the labels a and b represent two independent measurements). All light back-reflected (rays 1, 2) is fed into the two interferometer arms by a beam splitter. In the reference arm, an acousto-optic modulator (AOM, NEOS Model 26055) shifts the frequency of the light upwards by 55 MHz, corresponding to several periods within the short passage time (tens of microseconds) of the particles in the focus. The delay arm contains a motorized variable delay line (VDL, General Photonics VariDelay). The light from the two interferometer arms is recombined by another beam splitter/combiner and a broadband photo-receiver (New Focus Model 1811) serves as detector.

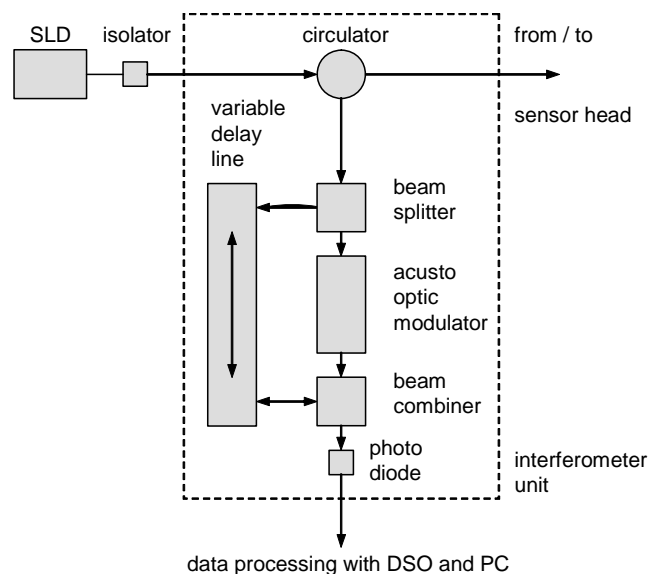


Figure 1: Schematic setup of optical components in the interferometer unit, which also includes the light source.

First, only consider one measurement, i.e., laser beam “a”. As shown in Fig. 2, the path length of ray 1a is longer than that of ray 2a. Denote the distance between the surface and the particle as D and the path lengths of both interferometer arms (between the two beam splitters/combiners) as l_{ref} and l_{delay} , respectively. If the VDL is set such that $l_{ref} + 2D = l_{delay}$ (“positive delay”), for example, the part of ray 1a going through the reference arm interferes with those parts of ray 2a which go through the delay arm. In a static situation the frequency of the AOM is now seen as beat signal at the detector. The same phenomena occurs if the VDL is set to $l_{ref} + 2D = -l_{delay}$ (“negative delay”). Then the part of ray 1a going through the delay arm interferes with the part of ray 2a which goes through the reference arm.

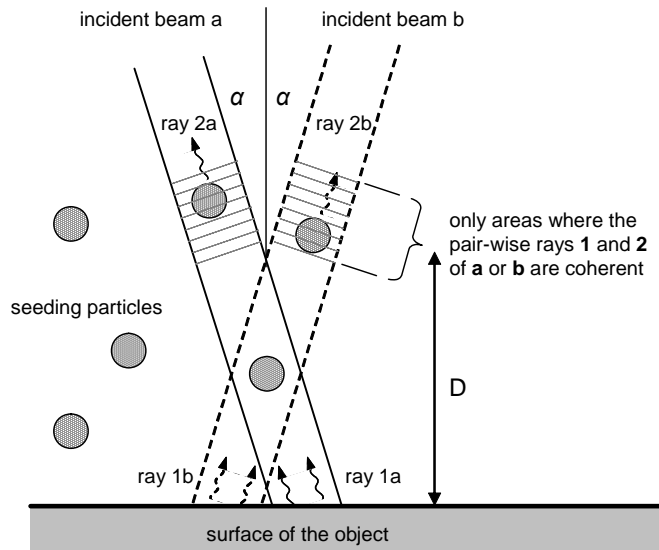


Figure 2: Schematic setup of the interaction between laser beam and particles.

With relative movement between the particle and the surface there is a frequency difference between rays 1a and 2a, which in case of interference results in a shift of the beat signal. The direction of the shift depends on the setup of the autocorrelator, positive or negative delay and of course it depends on the directions of the relative movements to each other (see Sect. 3).

In the absence of interference, no beat signal is present. This means that only those particles produce signals, which are within a thin layer from the surface. The thickness of the layer is approximately equal to half the coherence length of the light source, i.e., 30 micrometers.

The Doppler shift is proportional to the relative velocity between the particle and the surface along the propagation direction of the laser beam. Since the beam is not perpendicular to the surface, it depends on the wall-normal and the wall-parallel velocity. Note that a single beam is sufficient to measure one component of the velocity vector, unlike in LDV where a pair of laser beams is required for each component.

Now consider a second measurement where the SFE is rotated by 180°. The incident angle α of the laser beam “b” is then in the opposite direction. It will produce a Doppler-shifted beat signal whenever a particle crosses its path at the same distance D from the wall. But because beam “b” has the opposite incidence angle, the sign of the Doppler shift is reversed.

The distance between the measurement volume and the wall can be adjusted by adjusting the delay of the VDL – independent of the vertical position of the SFE. Irrespective of any movement of the surface, measurements are always performed at a set distance from the wall. One could say that the measurement location is in wall-fixed coordinates instead of lab-fixed coordinates as for other techniques.¹

As shown in Fig. 2, the measurement volumes of the two beams do not coincide exactly. Consequently, the beams do not look at the same horizontal position. But the spacing of the beams and their diameter is small and since the resolution in wall-parallel direction is usually not crucial, this should not pose a problem.

¹Strictly speaking this only refers to the wall-normal coordinate. The wall-normal and wall-parallel velocity, however, are both determined relative to the wall.

3. Data analysis SR-LDV

First, consider the wall-parallel velocity component u only and assume (without loss of generality) that the bisector of the laser beams is perpendicular to the wall. Interference between rays 1a and 2a produces a peak in the power spectrum at $f_a = u (2\sin(\alpha) / \lambda) + f_{AOM}$ (λ is the wavelength of the laser beams). The Doppler shift between rays 1b and 2b has the same magnitude, but opposite sign. The peak is thus at $f_b = u (2\sin(-\alpha) / \lambda) + f_{AOM}$. The difference between these two Doppler-peaks, as in LDV, is only proportional to u . Note, however, that this is twice the frequency shift measured by LDV. Next, consider the wall-normal velocity component v . For this case, the peaks from both beams are at the same frequency, which is different from f_{AOM} . The difference between the observed frequency and the AOM frequency is proportional to v .

Now consider a more general velocity vector $u = (u, v)$. The power spectrum will exhibit two peaks f_a and f_b . Denote the spacing of the two peaks as $\Delta F = |f_a - f_b|$ and the average Doppler-shift as $\Sigma F = (f_a + f_b) / 2 - f_{AOM}$. The velocity vector is then obtained from

$$u = \Delta F \cdot \lambda / 4\sin(\alpha) \quad \text{and} \quad v = \Sigma F \cdot \lambda / 2\cos(\alpha).$$

Finally consider the three-dimensional velocity vector $u=(u, w, v)$, where now u and w are parallel to the surface and v , as before, is the out-of-plane velocity component. The second in-plane velocity component w can be determined by another measurement essentially representing a third laser beam. This laser beam can also be obtained by rotating the SFE head by 90° .

Since α is small, the sensitivity to wall-normal velocities is much larger than to in-plane velocities (the ratio of the sensitivities is $1 / \tan(\alpha)$). This is desirable, because the wall-normal velocities are much smaller than the wall-parallel velocities in boundary layer type flows.

In order to relate the sign of the shift of the beat signal, $f - f_{AOM}$, to the flow direction, one has to account for the setting and for the design of the interferometer. With an interferometer design as shown in Fig. 1, consider a case where the light reflected off the particle is blue-shifted, i.e., $f_2 > f_1$ (where f_1 and f_2 are the frequencies of rays 1 and 2, respectively, as shown in Fig. 2). When the setup of the interferometer is such that the path lengths match when ray 2 passes through the AOM and ray 1 passes through the delay arm, i.e., to a negative delay, then the beat note will have the frequency $(f_{AOM} + f_2) - f_1$. When, on the other hand, ray 2 passes through the delay arm and ray 1 is frequency-shifted, then the beat note has the frequency $(f_{AOM} + f_1) - f_2$. For both scenarios the shift of the beat signal has opposite signs. The same case with an interferometer design where the AOM is included in the delay arm, will lead to beat signal shifts in the opposite direction.

It has been assumed that the orientation of the sensor head to the surface is known. Lacking the orientation of the wall relative to the detector the flow direction relative to the wall cannot be obtained. In this case only the flow velocities relative to the sensor head can be determined. Another assumption was that the wall is stationary. When the wall moves relative to the sensor head, the measured velocities are relative to the wall speed.

4. Measurement principle SR-L2F

The key features of this technique are the same as for the previous one, namely low-coherence velocimetry with spatial self-referencing capability. Now, however, two laser beams are used to measure a single velocity component. The standard laser-two-focus principle is based on the measurement of the time of flight of a particle between two light gates. The light gates are formed by two highly focused laser beams, which allow the detection of relatively small particles. The lengths of the focal regions are usually still several hundred micrometers, which limits the spatial resolution in the beam-wise direction. Also, the location of the focal region relative to an object is not known, but only relative to the focusing optic. Using low coherence light and an interferometer setup resolves both limitations. Only particles, which pass at a certain distance from the wall across the focal region produce a signal.

The changes to the experimental setup are twofold: First, the three-port polarizing independent circulator is replaced by a four-port polarizing circulator. It provides two independent beams of perpendicular polarization. The incoming light from these two both ports is directed into the interferometer.

In the SR-L2F setup both laser beams are set perpendicular to the surface. Therefore no Doppler-shift is generated by wall-parallel velocities. The extraction of velocity data follows straight forward common L2F analysis techniques, except that it handles the data from the beat signals. The measured velocities are then relative to the sensor head. Additionally, the system is sensitive to out-of-plane velocities by detecting the Doppler shift, as in SR-LDV.

5. Results

5.1 Signal processing

Fig. 3 shows the data acquisition chain used for the experiments in this paper. The analog signals from the photo-receiver are first filtered by a bandpass-filter (Mini Circuits BBP-60) and then amplified by 36 dB with a high speed amplifier (Hamamatsu C5594-12). The preconditioned signals are then digitized with 8 bit precision by a

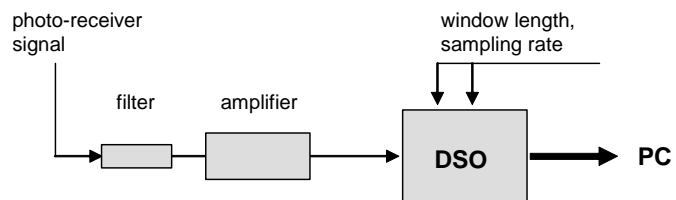


Figure 3: Data acquisition chain for Self-Referencing velocimetry experiments.

Digital Storage Oscilloscope - DSO (LeCroy LT347L). Data is then transferred to a PC through a 10 MBit Ethernet connection for further analysis and storage. The sampling rate and the acquisition window length are set through the DSO. The subsequent data analysis was performed by a LabView program (Ver. 7.1, National Instruments). The raw data is first bandpass filtered with a second-order Butterworth IIR-filter. For SR-LDV measurements, the maximum of the power spectrum is extracted by an interpolating peak-detection routine. In the L2F routine the beat note envelope is determined by a Hilbert transformation and a lowpass filter. Signals above a threshold are then indicated with 1 and below the threshold with 0. Next this binary signal is autocorrelated. In the autocorrelation function all peaks are detected and stored. The further statistical analysis was done in MatLab.

5.1. Closed rectangular channel

The tests in a closed rectangular channel were primary intended to demonstrate the performance of the measurement system under controlled conditions. Also comparisons with the known theoretical profile are possible. Tests with the SR-L2F setup provided additional and independent data for the velocity profile.

The channel is 20 mm wide, 500 mm long, and the parallel plates were 3.4 mm apart. The plates were made of Plexiglas, thus providing optical access. Oil (Bizol, CGPL-68) was sucked through the channel at a constant flow rate. Aluminum powder with particles sizes of approx. 10-100 microns was used as seeding. In both configurations the SR-LDV sensor head was placed approx. 6 cm above the channel. The diameter of the coupling lens was 5 millimeter. At the back side of second Plexiglas wall a retro-reflecting foil was affixed (see Fig. 4). The retro-reflector results in high back-reflection levels even at high incident angles. The reference location then was not the channel bottom, but the retro-reflector. Hence, the optical delay set in the interferometer representing the bottom wall is not zero.

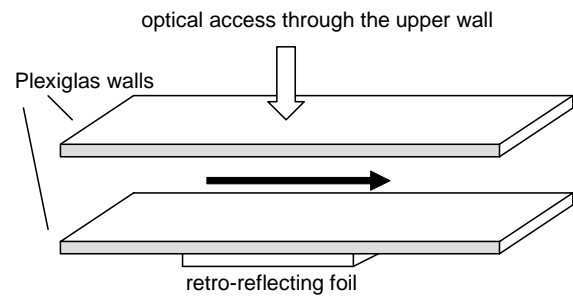


Figure 4: Schematic setup of the interaction between laser beam and particles.

In Fig. 5, which shows the comparison of the measured flow profiles, the positions in the channel were recalculated under the consideration of the refractive index of water and the mentioned offset. In the SR-LDV measurements the observation angle was +/- 14°, indicated with either *forward* (looking against the flow direction) or *backward* (looking in the flow direction). The optical delay

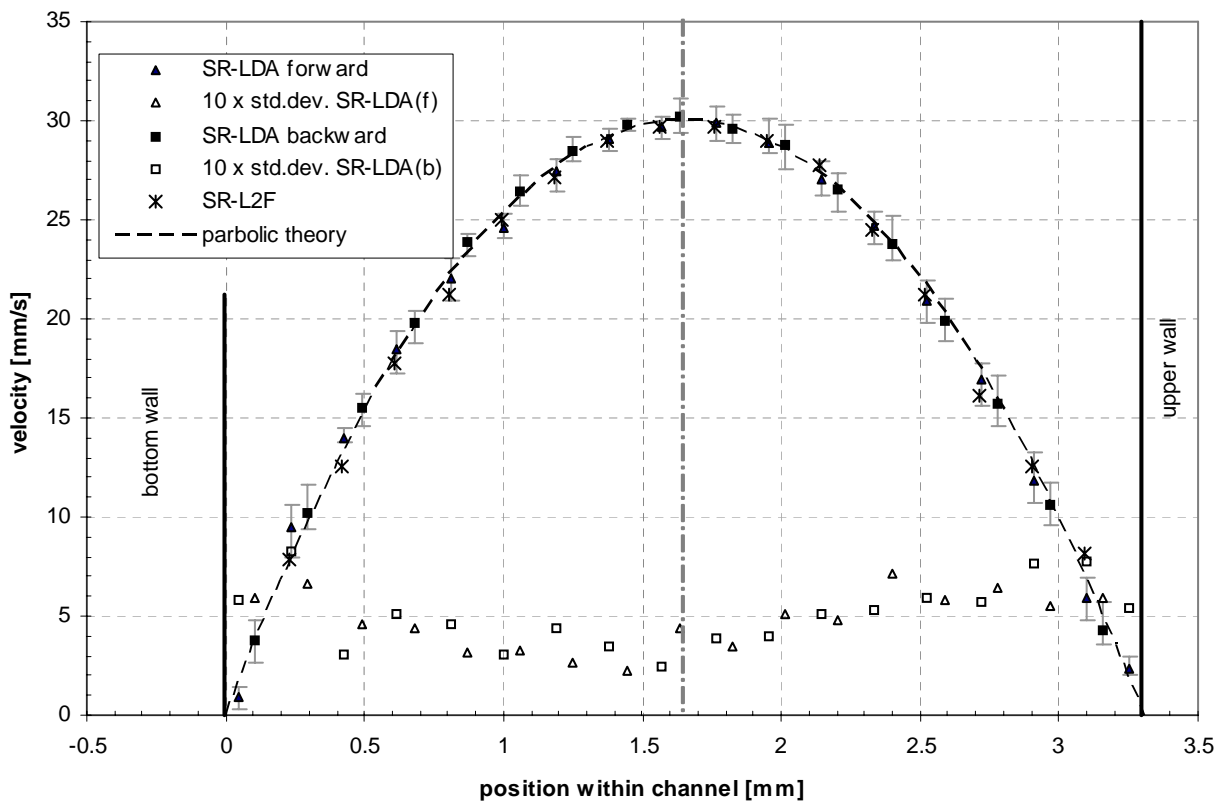


Figure 5: Measured flow profiles in a closed channel, comparison SR-LDV, SR-L2F and theory.

in the used autocorrelator (Fig. 1) was set to positive values. Therefore the observed beat signals are smaller than the AOM frequency for the forward setup and higher for the backward setup at positive flow directions. The error bars for SR-LDV representing the minimum and maximum velocity out of 20-50 measurements for each position. The standard deviation is with approx. 0.05 mm/s (200 Hz) nearly constant over the profile. All data was obtained at a sampling rate of 50 MHz and with a measurement window of 100k samples. Undersampling shifts the beat signal to 5 MHz. At low flow speeds close to the wall, the particle passage was longer than the acquisition window. The number of samples defines then the resolution of the power spectrum, i.e., in this test the resolution was 500 Hz. It seems that the frequency equivalent of the length of a given a beat signal, improved by a factor of 2 due to the interpolation scheme for the peak detection in the power spectrum, defines an upper bound for the system accuracy for a single measurement. Using forward and backward measured data together, as described in Sect.3, the resolution will be the same. Higher accuracies then only can be obtained with larger particles, i.e., longer particles passage times.

For the L2F measurement the plotted velocity at each position is based on the most probable time of flight (maximum of histogram). Both measurements methods show good agreement with the theoretical parabolic velocity profile.

5.2. Rotating cylinder

The tests at a rotating cylinder, i.e., Taylor-Couette flow, were performed to demonstrate the self-referencing capabilities. A metal cylinder (outer diameter of 83 mm) was placed coaxially in the center of a Plexiglas cylinder (inner diameter 89.3 mm, 5 mm thick). The length of both cylinders is approx. 30 cm, they were installed vertically. The resulting gap, of about 2.85 mm, was filled with olive oil and aluminum powder as seeding. The inner cylinder rotates with a frequency of up to 6 Hz.

The SR-LDV sensor head was placed approx. 6 cm away and set perpendicular to the cylinder axis. The optical front-end was tilted by a fixed angle against the flow direction. Therefore, only the circumferential velocities were investigated. Due to the curvature of the Plexiglas cylinder the value of this angle in respect to the surface of the inner cylinder cannot be clearly determined. The optical setup was fixed for the complete duration of the experiment and the observation angle then can be calculated from the known rotation speed of the cylinder. To obtain sufficient back-reflections from the surfaces at high observation angles, a retro-reflecting foil was affixed directly onto the rotating metal cylinder. As for the close channel experiments this means that the surface of the foil as reference is not identical with a zero delay in the interferometer.

The offset due to the path length within the reflector foil was measured to be 0.18 mm. This offset is not entirely unwelcome. Normally, measurements at or near the reference surface (within the first 50 to 100 μm) require that the path length through both interferometer arms are nearly equal. In that case, however, all other reflections also produce interference. This results in a high

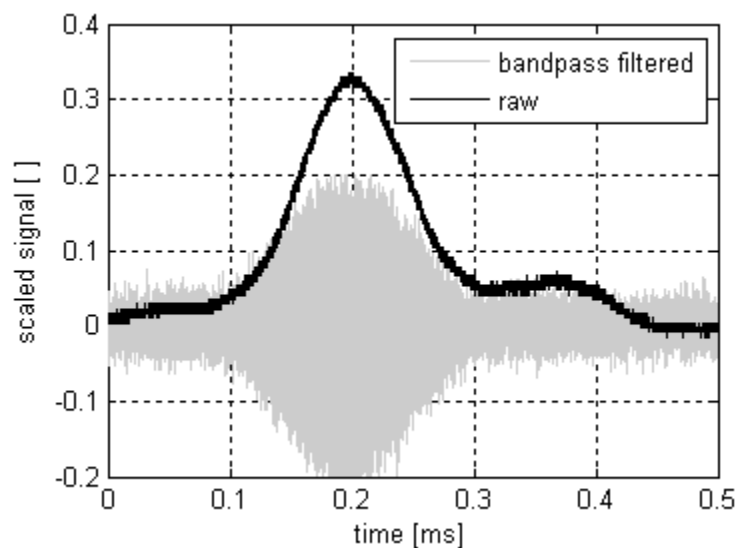


Figure 6: Particle passage: raw signal, filtered beat signal.

background level of the beat signal, above which passing particles cannot be detected. By offsetting the reference surface from the measurement volume, measurements are possible everywhere within the gap.

Owing to the spatially periodic structure of the retro-reflector, the back-reflection level is not constant, but instead highly modulated. It was also observed that, due to a shadowing effect, the reflection level from the retro-reflector and walls decreases during particle passages. However, in the bandpass filtered signal only the beat signals are visible (see Fig. 6).

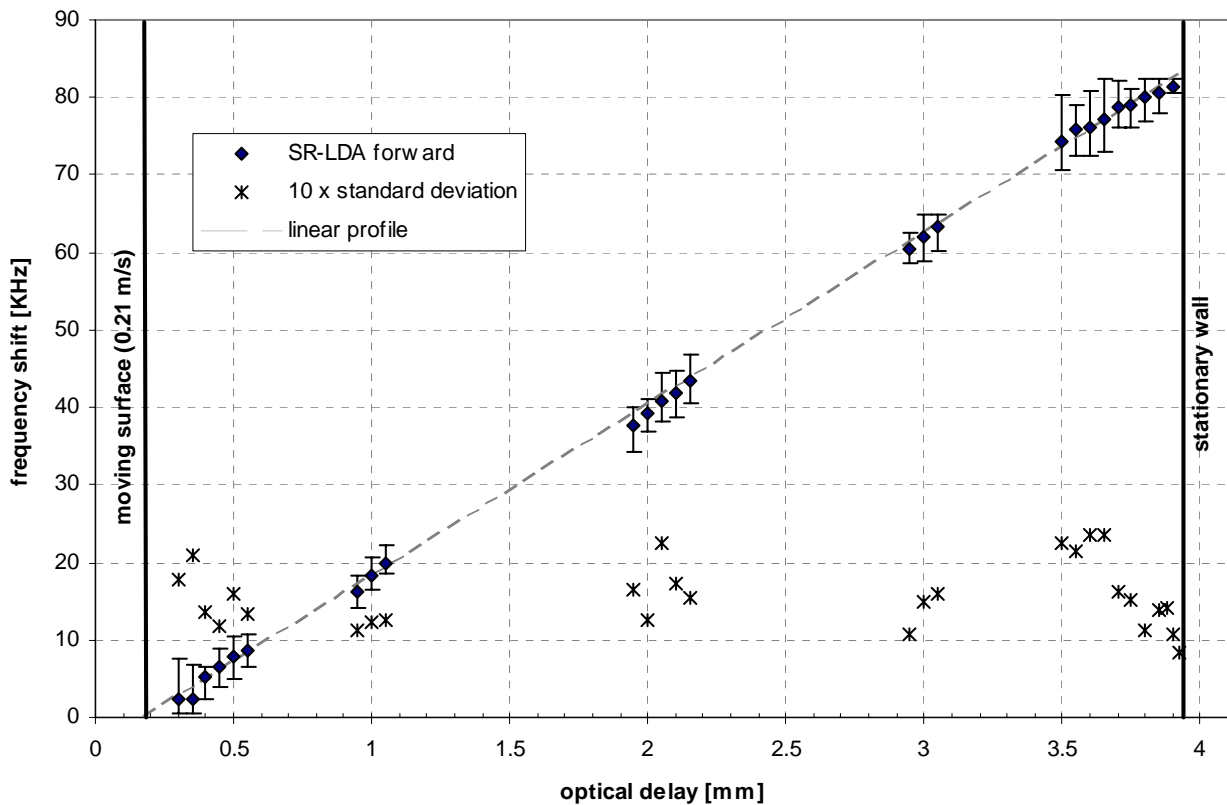


Figure 7: SR-LDV measured Taylor-Couette flow profile, $u_s = 0.21$ m/s.

In Fig. 7 the frequency-shift of the beat signal is plotted versus the optical delay of the autocorrelator. The surface velocity (u_s) of the inner rotating cylinder was 0.21 m/s. In a coordinate-system fixed with the rotating cylinder the fluid flow direction is negative, i.e., at the outer Plexiglas wall the relative velocity is the highest and at the moving cylinder surface zero, with a linear profile in-between. For positive optical delays and the forward setup this leads to a beat signal higher than the AOM frequency. The error bars represent the minimum and maximum of the frequency shifts out of 10 - 30 measurements for each position. The standard deviation is between 1 and 2 KHz and nearly constant over the profile. Data with high spatial resolution was obtained close to each surface and within three central regions. Close to the fix Plexiglas wall the data rate drops rapidly, because the absolute flow speed is close to zero and the number of particle passing the laser beam per unit time decreases.

Fig. 8 (upper panel) shows the frequency shift of the beat signal versus the optical delay of the autocorrelator at different rotations speeds of the cylinder. The data series are denoted by the surface speed of the rotating cylinder. The maximum rotation speed of this test setup was approx. 6 Hz, corresponding to a surface velocity of $u_s = 1.55$ m/s. The data at all rotation speeds shows a

linear behavior in accordance with theory. The errors over each profile are again nearly constant. The lower left panel of Fig. 8 shows the range of the measured frequency shifts and the standard deviation for each rotation speed. “max error” refers to the difference between the highest measured frequency shift and the mean, “min error” refers to the difference between the lowest frequency shift and the mean. These measures are shown averaged over the gap, because they are nearly constant for a given rotation speed. In the lower right panel of Fig. 8 these values are plotted relative to the surface velocity. These “ u_s -relative” errors are independent of the rotation speed. At all surface velocities, except at 1.55 m/s, the data was obtained at a sampling rate of 50 MHz and with a measurement window of 25k samples. At the highest rotational speed only 5000 samples have been recorded. Hence, the spectral resolution was 2 KHz and 10 KHz, respectively.

At the lowest rotation speed the beat signal length of all particle passages in the profile was similar to the length of the acquisition window. This is also true for particles passing closed to the outer wall. There the signal length is limited by the modulation of the reference signal from the retro-reflector. At higher rotations speeds the beat signal length was shorter than the acquisition

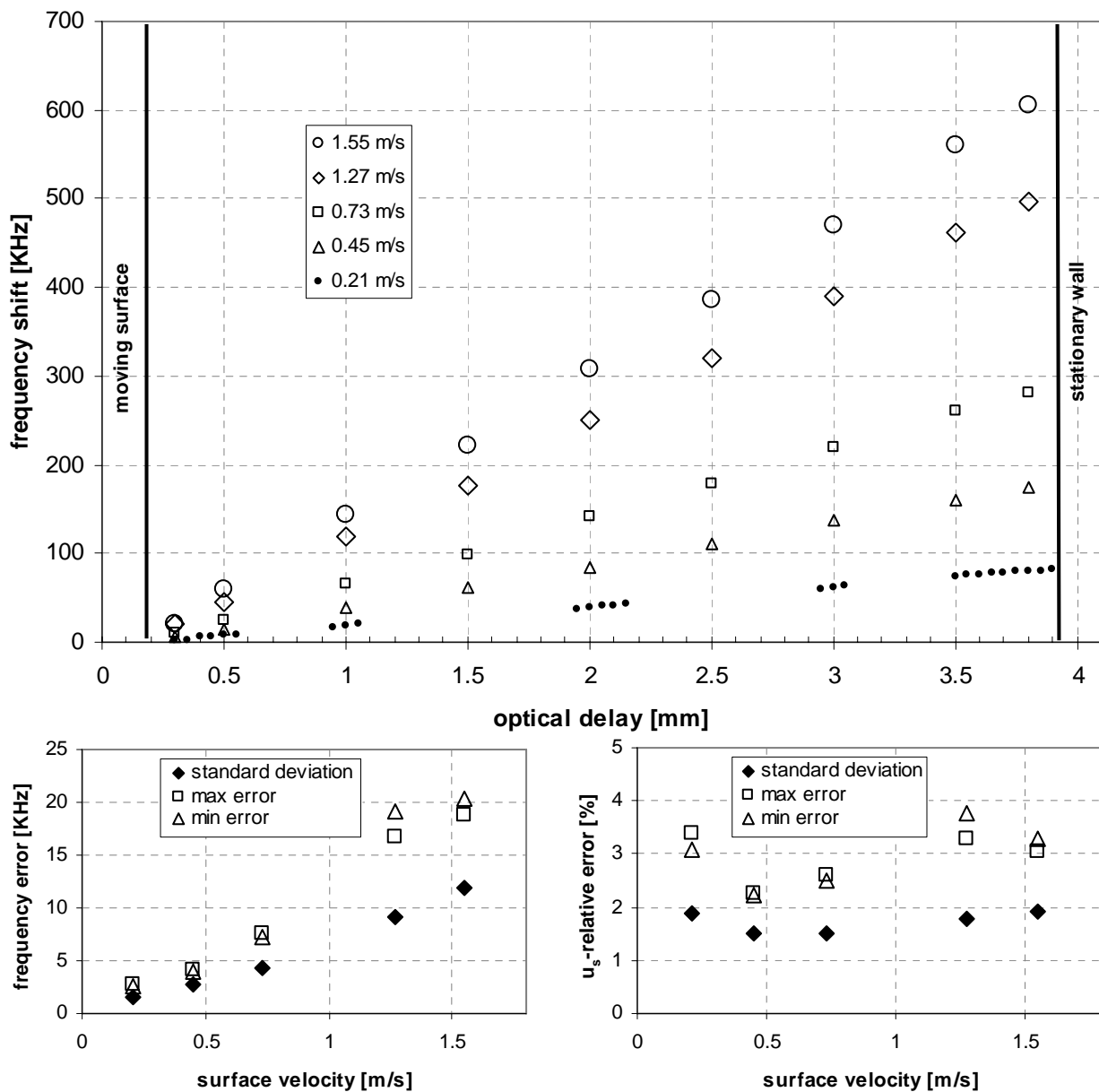


Figure 8: SR-LDV measured Taylor-Couette flow profiles at different surface velocities.

time, i.e., the real spectral resolution was lower. At a surface velocity of 1.55 m/s the beat signal lengths were again in the order of the acquisition window. Considering the modulation of the surface reflection the obtained accuracies are comparable to the tests in the closed channel.

L2F measurements at moving surfaces could not be performed. Due to the measurement principle single particles have to pass both light gates, as at the same time the reference reflection must be observed. With a modulated reference signal the probability of correlated signals drops rapidly, making L2F measurements impossible. With a mirror-like foil as reflector the reference signal was much more stable, but the data rate for L2F was still insufficient.

6. Conclusions

Two optical velocimetry techniques were presented which are based on low-coherence interferometry. Both have in common that the extent and the error of the location of the measurement volume are comparable to the coherence length of the light source (tens of micrometers). They also share the features that the measurement location is set relative to a reference surface (which could be the surface of a moving object), that they require particle seeding and that the measurement location can be scanned along a line without mechanical movement of the sensor head. Multiple components of the velocity vector can be measured using a single interferometer and light source.

Both techniques were demonstrated in proof-of-principle measurements for liquids. The measurement range depends on the power of the light source, the reflection levels off the reference surface and the particles (i.e., particle size), and the collection angle (= focusing angle) of the optics (i.e., lens diameter and distance to measurement volume). A lens with a diameter of 5 mm, a measurement distance of 60 mm (collection angle of approx. 5 deg.), aluminum powder for particle seeding, and a retro-reflector on the reference surface allowed a measurement range of 4 mm.

While a larger collection angle increases the sensitivity (allowing for smaller particles), this also increases the measurement uncertainty, because the uncertainty of the angle under which a particle is observed increases. In the present measurements, this source of noise was negligible compared to the spectral resolution, which depends on the length of a beat signal and the sampling rate. The frequency resolution could be improved by a factor of 2 by an interpolation scheme.

Current work focuses on making the techniques applicable for measurements in air. The experimental setup presented here yielded insufficient reflection levels from salt particles (typical diameter of 3 micrometer), even when using larger collection angles. Improvements were achieved using a mirror-like reference surface onto which a single laser beam is directed perpendicularly. This setup highly amplifies the interference signal between the dim reflections off the particles and off the reference surface (which almost saturates the photodetector), but only out-of-plane velocities can be detected. Adapting the setup to SR-L2F, i.e., using two laser beams, already lead to insufficient reflection levels. We anticipate further improvements by an order of magnitude by using a pulsed light source.

References

- Büttner L and Czarske J (2001) A multimode-fibre laser-Doppler anemometer for highly spatially resolved velocity measurements using low-coherence light. *Meas Sci Technol* 12:1891-1903
- Büttner L and Czarske J (2003) Spatial resolving laser Doppler velocity profile sensor using slightly tilted fringe systems and phase evaluation. *Meas Sci Technol* 14:2111-2120
- Hägmark CP, Bakchinov AA, Alfredsson PH (2000) Measurements with a flow direction boundary-layer probe in a two-dimensional laminar separation bubble. *Exp Fluids* 28:236-242
- Ligrani PM, Bradshaw P (1987) Spatial resolution and measurement of turbulence in the viscous sublayer using subminiature hot-wire probes. *Exp Fluids* 5:407-417
- Lin HJ, Perlin M (1998) Improved methods for thin, surface boundary layer investigations. *Exp Fluids* 25:431-444
- Meinhart CD, Wereley ST, Gray MHB (2000) Volume illumination for two-dimensional particle image velocimetry. *Meas Sci Technol* 11:809-814
- Schlichting H, Gersten K (2000) *Boundary-Layer Theory*. Springer Verlag, Berlin
- Wolff S, Brunner S, Fottner L (2000) The Use of Hot-Wire Anemometry to Investigate Unsteady Wake-Induced Boundary-Layer Development on a High-Lift LP Turbine Cascade. *J Turbomach* 122:644-650